Available online at www.sciencedirect.com
ScienceDirect
Applied Surface Science 254 (2008) 4965–4969
applied surface science
www.elsevier.com/locate/apsusc

Electron stimulated desorption of O_2^+ from gadolinia-doped ceria surfaces

Haiyan Chen [a], Alex Aleksandrov [a], Meilin Liu [b], Thomas Orlando [a,*]

[a] School of Chemistry and Biochemistry, Georgia Institute of Technology, 901 Atlantic Drive, N.W., Atlanta, GA 30332, United States
[b] School of Materials Science and Engineering, Georgia Institute of Technology, Atlanta, GA 30332, United States

Received 19 June 2007; accepted 29 January 2008
Available online 7 February 2008

Abstract

The interactions of gas phase oxygen with gadolinia-doped ceria (GDC) surfaces are investigated by electron stimulated desorption (ESD). The primary desorbed cationic species related to molecular oxygen adsorption is O_2^+. The threshold energy for ESD of O_2^+ is 13–14 eV, indicating electron impact ionization of molecular oxygen bound at oxygen vacancies. Dependence of O_2^+ velocities upon incident electron energy and substrate temperature reveals the dominant influence of the effective charge of the adsorption complex. The O_2^+ velocity distribution is bimodal, and the onset of the faster components at room temperature is related to the balance between fluxes of incident electrons and secondary electron emission, causing effective hole production and neutralization of trapped electrons at surface states.

PACS : 79.20.Kz; 81.05.Je

Keywords: Oxygen molecule; Gadolinia-doped ceria; Electron stimulated desorption

1. Introduction

Polycrystalline gadolinia-doped ceria (GDC) has been widely investigated as a promising low temperature solid oxide fuel cell (SOFC) electrolyte and as part of composite electrodes to facilitate ionic conduction within the electrodes [1–4]. Raman spectroscopy indicated that oxygen readily adsorbs on the surfaces of a partially reduced ceria [5] and the adsorption of oxygen at various surface sites is the first step toward oxygen reduction. Since GDC has the same structure as that of CeO_2 (fluorite), knowledge on the interaction of oxygen with CeO_2 surfaces may help the investigation of O_2 adsorption on GDC. An understanding of molecular oxygen interactions with GDC surfaces may provide insight into the oxygen reduction process at electrode/electrolyte interfaces, thus providing scientific guidance for rational design of better electrodes. The main difference between GDC and CeO_2, however, is that Gd^{3+} is not active in electron transfer while cerium can change its oxidation state readily between Ce^{3+} and Ce^{4+}.

The interactions of molecular oxygen with transition metal oxide surfaces are important in many processes involving oxygen reduction or catalytic oxidation. Various intermediates from physically adsorbed oxygen, superoxide (O_2^-), peroxide (O_2^{2-}), to O^- can be formed before oxygen is reduced to lattice O^{2-}. For ceria, molecular oxygen presumably adsorbs at oxygen vacancy sites on partially reduced surfaces, but the exact adsorption state is not very clear [6]. Temperature programmed desorption (TPD) studies indicate that weakly bound oxygen desorbs on ceria films at 800–1250 K [7]. Electron paramagnetic resonance (EPR) and Fourier transform infrared (FTIR) studies show that a variety of paramagnetic superoxide radical species can be detected on many metal oxide surfaces [8] and on polycrystalline ceria surfaces [9,10]. The EPR signal of superoxide species on ceria surfaces can be grouped into two types, one is thought to be related to isolated oxygen vacancies and the other to aggregated oxygen vacancies. The bonds between the superoxide and the surface have different degrees of covalency but the exact picture of charge localization is not completely clear. UV irradiation of CeO_2 nanoparticles [11] and CeO_2/TiO_2 [12] in the presence of oxygen greatly increases the amount of superoxide radicals. These studies were performed with an ex situ procedure and

* Corresponding author. Tel.: +1 404 385 2243; fax: +1 404 894 7452.
E-mail address: Thomas.Orlando@chemistry.gatech.edu (T. Orlando).

0169-4332/$ – see front matter © 2008 Elsevier B.V. All rights reserved.
doi:10.1016/j.apsusc.2008.01.146

neither physically adsorbed O_2 nor O_2^{2-} species were observed by EPR or FTIR.

An in situ Raman spectroscopy investigation of O_2 adsorption on polycrystalline CeO_2 surfaces [13] revealed the physical adsorption of O_2 at 93 K and two types of O_2 chemisorption states associated with various oxygen vacancy sites. These include isolated oxygen vacancies and vacancy clusters. The non-dissociatively chemisorbed oxygen species can be designated as O_2^- or O_2^{2-}, depending on the cations they are associated with. The thermal stability of O_2^{2-} is higher than O_2^-, and the lifetime of the oxygen species on the surface is not known. The O_2 species are stabilized by the cations in the vicinity but the overall interaction is weak.

Electron stimulated desorption (ESD) is a surface specific technique that can provide valuable information concerning surface and adsorbate structures [14]. The conventional scheme for ESD studies of gas–solid interactions is to directly investigate the adsorbate–substrate complex. This method has yielded important information on systems such as H_2/TiO_2 (0 0 1), NH_3/TiO_2 (1 1 0), SO_2/TiO_2 (1 1 0), CO/TiO_2 (1 1 0), and NO/TiO_2 (1 1 0) [15]. However, this method only probes adsorbed species with long lifetimes. Information on the dynamic gas-phase interaction with the surface is completely lost. Our recent application of ESD to GDC [16–18] has established a fundamental understanding of the GDC surfaces and has set a foundation for exploration of the interactions between GDC and oxygen.

In this paper, we present an ESD study of non-dissociative adsorption of molecular oxygen on polycrystalline gadolinia-doped ceria surfaces. The electron stimulated desorption of O_2^+ is shown to originate from the GDC surfaces during O_2 adsorption. The influences of incident electron energy and substrate temperature on yields and velocity distributions are also presented. The mechanism of O_2^+ desorption is discussed in terms of ionization of various oxygen adsorption states.

2. Experimental

The details of $Ce_{0.9}Gd_{0.1}O_{2-\delta}$ (GDC) sample preparation and characterization by X-ray diffraction and scanning electron microscopy are reported elsewhere [16,17]. The GDC samples used in this study have a polycrystalline fluorite structure and a significant number of grain boundaries. The dimensions of the GDC pellet were about 10 mm × 6 mm × 1 mm.

ESD measurements were performed in an ultrahigh vacuum system with a base pressure of 2×10^{-10} Torr. The system is equipped with a quadrupole mass spectrometer (QMS), a time-of-flight (TOF) mass spectrometer, a pulsed low-energy electron gun, a calibrated dosing system, and a sample manipulator with temperature control in the range 100–900 K.

The GDC sample was mounted on a molybdenum plate and was annealed to 700 K to remove all contaminants from the surface. The oxygen used is from Matheson with a purity of 99.998%. The sample was irradiated by the pulsed electron beam at 1000 Hz with an electron flux of 10^{14} electrons/cm^2 s during a given pulse or time-averaged currents of 200 pA to a few nano-Ampere depending on the pulse width. Emitted cations were collected by applying a −50 V pulsed extraction potential to the TOF front lens assembly. To avoid the influence of the extracting field on the electron beam energy, the extraction potential was applied after the end of the electron pulse. For mass resolved ESD measurements, the QMS was employed as the mass analyzer, and was operated with its ionizer turned off. In general, three ESD–TOF spectra were taken at each electron energy and the average yield was used for threshold measurements. The yields were normalized to the electron beam current measured by a Faraday cup.

3. Results and discussion

3.1. Electron stimulated desorption of O_2^+

Typical TOF spectra of ions desorbed from gadolinia-doped ceria surfaces during pulsed electron irradiation at room temperature are presented in Fig. 1. The dominant ESD product from GDC in vacuum $\sim 10^{-10}$ Torr is H^+, represented by a single peak with a ~3 μs flight time. If oxygen is dosed above GDC surfaces and a pressure of $\sim 10^{-9}$ to 10^{-7} Torr is maintained, two new peaks with 15.7 and 16 μs flight times are observed when the sample is irradiated by electrons with energy above 50 eV. If the extraction potential is increased, the two peaks merge into one peak with a mass ~32 amu, indicating that they arise from ions of the same mass but different velocities. Assignment of both peaks to the same mass (32 amu) is also confirmed by quadrupole mass spectrometry. The two peaks are therefore attributed to O_2^+ molecular ions with different velocities and denoted as O_2^+(f)—"fast" and

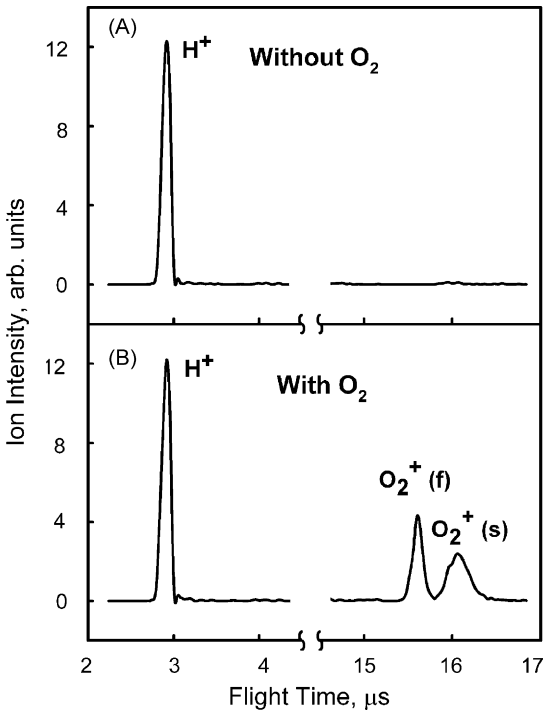

Fig. 1. The ESD–TOF spectrum of ions from a GDC surface at 2×10^{-10} Torr (panel A), and in the presence of 5×10^{-8} Torr of gas phase O_2 (panel B). The incident electron energy is 65 eV, the electron beam pulse width is 200 ns, substrate temperature is 300 K, and the extraction potential is −50 V.

O_2^+(s)—"slow". Most of the kinetic energy, obtained by the O_2^+ ions, results from their acceleration in the pulsed extraction field. At relatively low extraction potentials this energy can be comparable with the energy acquired by ions directly in the ESD process, and the flight time is significantly influenced by their initial kinetic energy.

The ESD of O_2^+ was previously observed from the O_2/Si (1 1 1) surface [19] with a kinetic energy of 2 eV and also from the O_2/K/Ru (0 0 1) system after oxygen dosing [20]. To our knowledge, no O_2^+ ESD has been reported from oxygen/metal oxide interactions. Photo-stimulated desorption of neutral O_2 from $YBa_2Cu_3O_{7-x}$ by core level excitation is known, though no O_2^+ desorption was observed [21].

Our experiments on GDC show that if oxygen is completely removed from the system the O_2^+ ESD yield is reduced by more than two orders of magnitude. This decreased process efficiency suggests that the O_2^+ emission may originate from short-lived intermediate adsorption states of oxygen on the GDC surfaces. It should be also expected that at an oxygen pressure 5×10^{-8} Torr, at least part of the detected O_2^+ ions can be created by O_2 ionization directly in the gas phase. To determine the gas phase contribution, the O_2^+ TOF spectra were measured at an O_2^+ pressure of 5×10^{-8} Torr with the GDC sample removed from the path of the electron beam. Comparison of this spectrum with the TOF spectrum of GDC, measured in the presence of O_2 at the same pressure, reveals significant differences. In the case of O_2 ionization in the gas phase, the O_2^+ is represented by only one peak with an amplitude an order of magnitude smaller than that observed in the case of GDC irradiation.

As mentioned above, part of the O_2^+(s) is always observed in the TOF spectra. This is independent of the presence of the sample in the path of the electron beam and is proportional to the O_2 pressure. Above 50 eV, the O_2^+(s) flight time and intensity does not depend on the electron energy and the sample temperature, though it depends on the sample position. Therefore, the O_2^+(s) in the TOF spectrum using incident electrons >50 eV is assigned to O_2 ionized in the gas-phase in front of the sample. Assuming that electron impact ionization cross-sections of oxygen molecule in the gas and in the adsorbed state are approximately the same, the concentration of O_2 adsorbed on the GDC surfaces can be evaluated using the TOF peak area ratios. Since the signal from the adsorbed phase is about 5 times higher than from the gas, the calculated equilibrium concentration of adsorbed molecules an O_2 pressure of 5×10^{-8} Torr is $\sim 10^{10}$ molecules/cm^2, and the average adsorption time $\sim 5 \times 10^{-4}$ s.

3.2. Influence of electron energy and temperature on O_2^+ ESD

The influence of the incident electron energy (E_i) on the O_2^+ ESD from GDC surfaces in the presence of adsorbed oxygen is shown in Fig. 2. In the range of E_i from 15 to 55 eV, only one O_2^+(s) desorption peak (flight time ~16 μs) is observed. At energies above 45 eV, this peak broadens and its position shifts to shorter flight times. When the electron energy reaches 60 eV, a new O_2^+(f) peak with flight time ~15.7 μs appears and the intensity of the O_2^+(s) peak at 16 μs decreases 4–6 times. With increasing E_i, the O_2^+(f) peak position gradually shifts to shorter times, its intensity decreases and halfwidth grows. Finally, at electron energies above 100–150 eV, the O_2^+(f) peak splits into two components with flight times around 15.3 and 15.5 μs. Contrary to the O_2^+(f), the intensity and position of the O_2^+(s) peak in the energy range 60–200 eV remains approximately unchanged.

A summary of the influence of E_i on O_2^+(s) and O_2^+(f) yields is presented in Fig. 3. The yields are calculated as the TOF signal integrated over time in the range from 15.1 to 15.7 μs for the fast component and from 15.7 to 16.7 μs for the slow component. The O_2^+(s) yield increases with electron energy from a 13 to 14 eV threshold, reaches maximum at ~50 eV, and decreases rapidly from 50 to 80 eV. The drop of the O_2^+(s) yield at $E_i > 50$ eV correlates with the sharp increase of the O_2^+(f) component, indicating transformation of the adsorption complex responsible for O_2^+(s) desorption into the form emitting O_2^+(f). An alternative explanation that O_2+(f) production above $E_i = 50$ eV is due to a mechanism involving multielectron excitations rather than by structural changes of an adsorption complex is not supported by the data obtained at higher temperatures. At energies $E_i > 80$ eV, the peak position and intensity of the O_2^+(s) are constant, independent of E_i and sample temperature. Contrary to the slow component, the spectrum of the fast component continues to change with electron energy above 50–70 eV. At $E_i > 70$ eV the overall

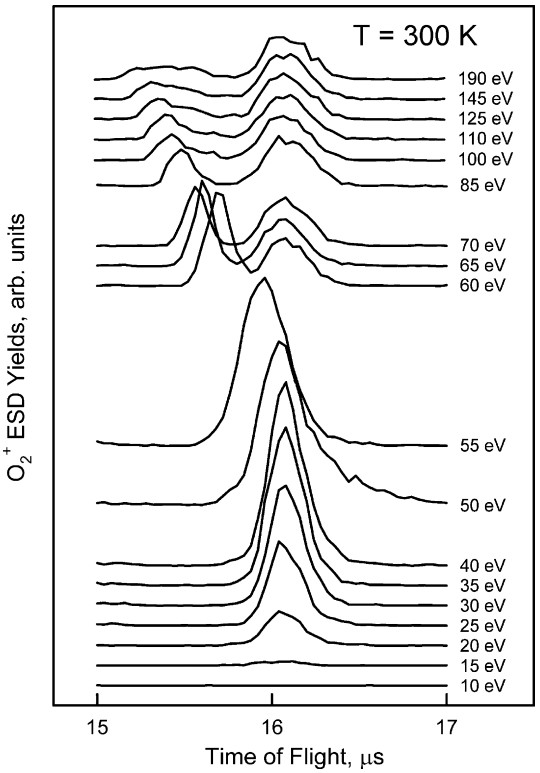

Fig. 2. TOF spectra of O_2^+ ESD from the GDC surface with adsorbed molecular oxygen as a function of incident electron energy. The substrate temperature is 300 K, the electron beam pulse width is 200 ns, and the pressure of oxygen is 5×10^{-8} Torr.

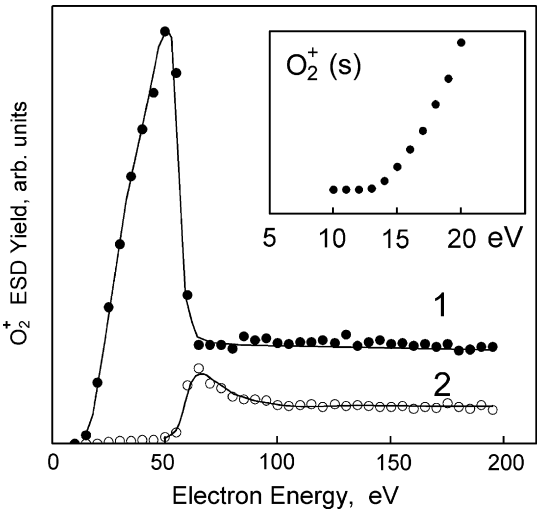

Fig. 3. Electron energy dependence of oxygen O_2^+(s) (1, solid circles) and O_2^+(f) (2, opened circles) ESD yields. The electron pulse width is 200 ns, substrate temperature is 300 K, and the oxygen pressure is 5×10^{-8} Torr.

number of emitted O_2^+(f) ions remains constant. The energy dependence of both the fast and the slow components are very different from that observed for the ionization of gas phase O_2 [22]. In particular, no extrema of ionization cross-section are present in the gas phase data.

The O_2^+ ESD threshold is measured and presented in the inset of Fig. 3. The experimental value is ~13 eV, which is not close to any of the core levels of Gd 5p (23.0 eV) [23], Ce 5p (18.0 eV) [24] or O 2 s (21.8 eV) [24]. Therefore, the ESD of O_2^+(s) cannot be explained by ionization of core level electrons of the metal oxide. In fact, this threshold is rather close to the ionization potential of molecular oxygen (12.06 eV), indicating that the O_2^+ desorption most likely originates from the electron impact ionization of the adsorbed molecular oxygen species.

To examine the O_2 interactions on GDC surfaces near fuel cell operating temperatures, we measured the yields and velocity distributions as function of E_i at 560 K. O_2^+ ESD–TOF spectra obtained at 560 K is presented in Fig. 4. This data is different from those obtained at room temperature in several ways. At 560 K, the flight times of both O_2^+ components do not shift with electron energy. The splitting of the fast O_2^+ component at high electron energies does not occur, indicating that at elevated temperatures only one form of O_2 adsorption is stable. At electron energies below 50 eV, the O_2^+(s) yield is ~5 times lower and the O_2^+(f) yield is much higher than at 300 K. In Fig. 5, no extremum of the O_2^+(s) yield vs. E_i is observed. The O_2^+(s) band intensity increases with the incident electron energy and at $E_i > 70$ eV reaches the same level which is observed for 300 K. Such behavior implies that at 560 K, most of the O_2^+(s) originates from ionization of oxygen in the gas-phase. The O_2^+ ESD yields presented in Fig. 5 also show that at high temperature, the threshold energy of the fast component is the same as of the slow one. The O_2^+(f) threshold is shifted to ~13 eV instead of the ~40 eV onset observed at room temperature. At 560 K and $E_i < 50$ eV, the O_2^+(f) ESD is greatly enhanced and the O_2^+(s) is suppressed compared to the room temperature data. This implies that some adsorption

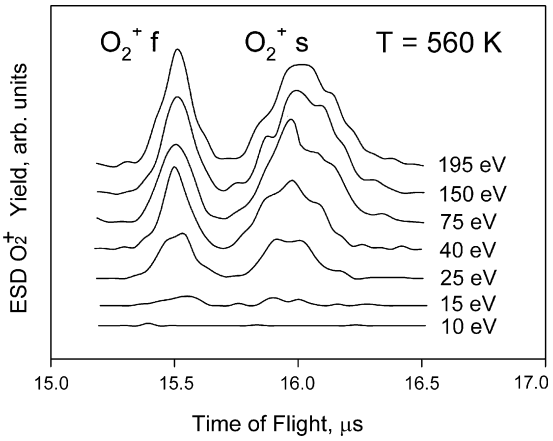

Fig. 4. TOF spectra of O_2^+ ESD from the GDC surface with adsorbed oxygen at different incident electron energies, at temperature 560 K. The pulse width is 200 ns, and the pressure of oxygen is 5×10^{-8} Torr.

complexes leading to O_2^+(s) ESD at low temperature convert into the form emitting O_2^+(f) at 560 K.

3.3. Types of adsorption complexes and O_2^+ ESD mechanism

Previous investigations have demonstrated that at room temperature, molecular oxygen does not interact with a perfect metal oxide surface, but chemisorbs at defect sites, especially oxygen vacancies (Va). Thus, the chemically adsorbed oxygen intermediates bound to oxygen vacancies are considered to be primary precursors for O_2^+ ESD. High resolution scanning tunneling microscopy and density functional calculations show that at oxygen vacancy sites on CeO_2 (1 1 1) surfaces, the electrons released by oxygen are localized on lattice cerium ions adjacent to the vacancy [25]. When molecular oxygen is in contact with the surface of a metal oxide, the formation of O_2^- can occur. Electrons from partially reduced metal cations, electrons trapped by oxygen vacancies, or electrons induced by photon irradiation [26], can be transferred to molecular oxygen to form a superoxide anion. Since the electron affinity of the oxygen is positive (0.44 eV), the electrostatic contribution to

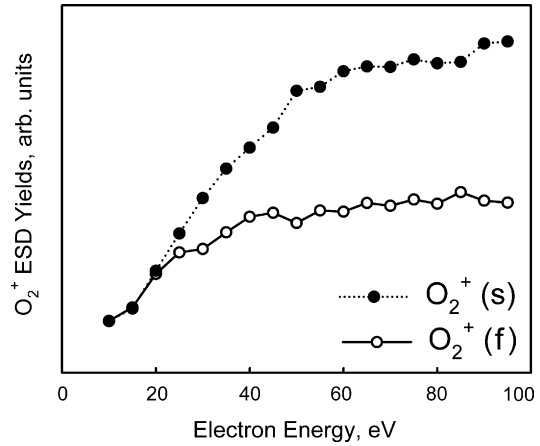

Fig. 5. Electron energy dependence of O_2^+ ESD at 560 K. The pulse width is 200 ns and the pressure of oxygen is 5×10^{-8} Torr.

the stabilization of the anionic species on the positive sites at the surface can play a fundamental role.

Molecular oxygen adsorbed on a vacancy cannot be ionized to O_2^+ by capturing a hole from the upper valence band. To remove an electron from O_2 (or 2 electrons from an $O_2{:}V_a^{++} + 2e$ adsorption complex) either external energy should be acquired directly by the adsorbate or a hole at a level deeper than the valence band should appear on one of the neighboring ions. Since the core ionization of crystal lattice ions requires at least 40 eV and the observed threshold for O_2^+ ESD is ~13 eV, electron impact ionization of the adsorbed O_2 or $O_2{:}V_a^{++} + 2e$ adsorption complex at energies below 45 eV should be the main ESD mechanism.

Once produced, the O_2^+ can be ejected from the surface by the Coulomb repulsion and acquire kinetic energy mainly according to the effective charge of the rest of the adsorption complex. If the local surface potential is close to neutral, the O_2^+ kinetic energy should be close to thermal. Higher kinetic energy is expected from the adsorption complex with the higher positive charge. Every process that changes the effective charge of the complex should influence the O_2^+ kinetic energy.

In general, the ESD efficiency increases with incident electron energy and concentration of adsorbed species. The dependence of the O_2^+(s) yield on incident electron energy presented in Fig. 3 demonstrates the opposite—suppression of O_2^+(s) ESD when the energy increases above 50 eV.

Our previous investigation of electron induced charging of GDC surfaces shows that at room temperature, and lower E_i, trapped electrons dominate at the surface. At higher energies, the concentration of trapped holes at the surface is higher [17]. At low E_i, trapped electrons decrease the positive charge of the vacancy and therefore the emission of slow O_2^+ is favored. Increasing the incident electron energy above 45 eV leads to the significant enhancement of the secondary electron emission, due to ionization of core levels of the crystal-forming ions—cerium (5 s level of Ce^{4+} in CeO_2, 37 eV [24]) and gadolinium (5 s level of Gd^{3+} in Gd_2O_3, 46 eV [23]). Emission of electrons from the surface creates uncompensated holes which can localize or interact with adsorption centers responsible for O_2^+(s) and change both the local structure and charge of the adsorption complex and the average, long-range surface potential. Above 50–60 eV, nearly all O_2^+(s) adsorption centers are destroyed by recombination with the holes, the overall concentration of the adsorbed oxygen is decreased, and a new type of center emitting O_2^+(f), becomes dominant. Multi-hole generation by core level Auger cascades can facilitate the emission of O_2^+ with even higher kinetic energy and a gradual shift of the flight time which is observed at $E_i > 50$ eV.

For the O_2^+ energy dependence at high temperature, the lower onset energy for the fast component can be explained by thermally activated excitation of electrons from the defect states. This process leaves the adsorption complex with one electron less or more positively charged, triggering emission of an O_2^+(f) component even at low incident electron energies. Under these conditions, hole creation by secondary electron emission is not yet a dominating process.

4. Conclusions

Investigation of O_2^+ electron stimulated desorption from gadolinia-doped ceria surfaces after molecular oxygen adsorption reveals the presence of two main components that differ in kinetic energy and originate from adsorption sites with different effective charges. The ~13 eV O_2^+ ESD threshold supports a mechanism that O_2^+ desorption mainly occurs from electron impact ionization of adsorbed O_2 or an $O_2{:}V_a^{++} + 2e$ adsorption complex. Analysis of the data collectively showed that the dominant adsorption complexes and emitted ion kinetic energies are defined by the state and charge of the solid surface. These depend upon the sample temperature, incident electron energy and secondary electron yield.

Acknowledgements

The authors thank Dr. Shaowu Zha for the preparation of GDC samples. This work was supported by the United States Department of Energy USDoE-NETL SECA Core Technology Program under Grant No. DE-FC26-02NT41572.

References

[1] C. Xia, M. Liu, Solid State Ionics 144 (2001) 249.
[2] C. Xia, M. Liu, Solid State Ionics 152–153 (2002) 423.
[3] B.C.H. Steele, Solid State Ionics 129 (2000) 95.
[4] H. Inaba, R. Sagawa, H. Hayashi, et al. Solid State Ionics 122 (1999) 95.
[5] S.B. Adler, Chem. Rev. 104 (2004) 4791.
[6] A. Trovarelli, in: G.J. Hutchings (Ed.), Catalytic Science Series, vol. 2, Imperial College Press, 2002, p. p. 508.
[7] E.S. Putna, J.M. Vohs, R.J. Gorte, J. Phys. Chem. 100 (1996) 17862.
[8] M. Labanowska, Chemphyschem 2 (2001) 712.
[9] X. Zhang, K.J. Klabunde, Inorg. Chem. 31 (1992) 1707.
[10] I. Colera, E. Soria, J.L. de Segovia, et al. Vacuum 48 (1997) 647.
[11] M.D. Hernandez-Alonso, A.B. Hungria, A. Martinez-Arias, et al. Appl. Catal. B: Environ. 50 (2004) 167.
[12] J.M. Coronado, A. Javier Maira, A. Martinez-Arias, et al. J. Photochem. Photobiol. A: Chem. 150 (2002) 213.
[13] V.V. Pushkarev, V.I. Kovalchuk, J.L. d'Itri, J. Phys. Chem. B 108 (2004) 5341.
[14] R.D. Ramsier, J.T. Yates Jr., Surf. Sci. Rep. 12 (1991) 243.
[15] J.L. de Segovia, E.M. Williams, Chem. Phys. Solid Surf. 9 (2001) 608.
[16] H. Chen, A. Aleksandrov, Y. Chen, et al. J. Phys. Chem. B 109 (2005) 11257.
[17] H. Chen, Y. Chen, A. Aleksandrov, et al. Appl. Surf. Sci. 243 (2005) 166.
[18] H.Y. Chen, A. Aleksandrov, S. Zha, et al. J. Phys. Chem. B 110 (2006) 10779.
[19] K. Sakamoto, K. Nakatsuji, H. Daimon, et al. Surf. Sci. 306 (1994) 93.
[20] G.H. Rocker, C. Huang, C.L. Cobb, et al. Surf. Sci. 250 (1991) 33.
[21] R.A. Rosenberg, C.R. Wen, Phys. Rev. B 37 (1988) 9852.
[22] E. Krishnakumar, S.K. Srivastava, Int. J. Mass Spectrom. Ion Process. 113 (1992) 1.
[23] D. Raiser, J.P. Deville, J. Electron Spectrosc. Relat. Phenom. 57 (1991) 91.
[24] Y.A. Teterin, A.Y. Teterin, A.M. Lebedev, et al. Radiochemistry (Moscow) 40 (1998) 101 (Translation of Radiokhimiya).
[25] F. Esch, S. Fabris, L. Zhou, et al. Science (Washington, DC, United States) 309 (2005) 752.
[26] M. Anpo, N. Aikawa, Y. Kubokawa, et al. J. Phys. Chem. 89 (1985) 5017.